Proceedings of ASME Turbo Expo 2011
GT2011
June 6-10, 2011, Vancouver, British Columbia, Canada

GT2011-45041

ADJOINT-BASED FLOW SENSITIVITY ANALYSIS USING ARBITRARY CONTROL SURFACES

Christian Frey*, Graham Ashcroft, Jan Backhaus, Edmund Kügeler and Jens Wellner
Institute of Propulsion Technology
German Aerospace Center (DLR)
Linder Höhe, 51147 Cologne
Germany
Email: Christian.Frey@dlr.de

ABSTRACT

This article describes how to extend the dsicrete adjoint method to functionals that are evaluated on arbitrary rotational control surfaces that intersect the flow domain at a position specified by the user, e.g. the pressure loss coefficient of a single blade in a multi-stage configuration. The definition and implementation of the mixed-out states on such surfaces is revisited.

The calculation of the corresponding right-hand sides in the adjoint system is explained. These techniques can be used to specify functionals that quantify the deviation of the radial distribution of the flow angles, relative mass flow, etc. from a given target distribution. Sensitivity studies using the conventional approach, i.e. by means of finite differences of many steady solutions, are compared to results based on the adjoint method. The applications demonstrate that the agreement between adjoint and conventional sensitivity predictions is excellent, if the exact definition of the surface functionals is taken into account.

NOMENCLATURE

CEV	constant eddy viscosity
F_j	flux through face j
I	objective functional
$MS(f-f^*)$	mean square deviation
R	residual vector
$S, \widetilde{S}$	source terms
T	temperature
$T_\mathbf{t}$	stagnation temperature
U	velocity
V_i	volume of cell i
div	divergence
$\dot{m}$	mass flow
n	surface normal vector
p	pressure
q	vector of conservative variables
x, r, ϑ	cylindrical coordinates
Γ	analysis surface
α_j	j-th design variable
β	circumferential flow angle
κ	thermal conductivity
λ	stagger angle
$\pi_\mathbf{t}$	stagnation pressure ratio
ψ	adjoint solution
ρ	density
$\vartheta_\mathbf{t}$	stagnation temperature ratio

INTRODUCTION

Computational fluid dynamics (CFD) is often used to understand flow phenomena for one given design, e. g. a turbomachinery configuration at a certain number of operating points. In that case, the role of CFD is primarily to give, as accurately as possi-

*Address all correspondence to this author.

ble, quantitative and qualitative information about the flows. On the other hand, many CFD applications take place in a context where, instead of only one isolated geometry, one considers a variety of designs, which is the case in aerodynamic design and optimization. Similarly, when a manufacturing tolerance is to be specified from an aerodynamic point of view virtually all possible manufacturing errors must be taken into account.

As computational power becomes more and more affordable, a conceptually simple approach to this problem can be the repeated use of a flow solver for many configurations. However, denoting by f the dimension of the design space, at least f calculations are needed to approximate a performance functional linearly, i.e. to calculate the gradient for one set of design variables. One may overcome this dilemma by the use of optimal control theory which suggests that instead of solving the primal equations, i.e. the flow equations, many times, one should preferably solve a dual system of equations. The dual system needs to be solved only once for each functional in order to determine the gradient for arbitrarily many design parameters. Moreover, its solution is roughly as difficult as the linearization of the primal equation, generally not more complex than one solution of the flow equations. It follows that, if far fewer functionals are used to assess the performance than there are geometric parameters, then the dual approach outperforms the primal approach dramatically. In the context of partial differential equations, the dual problem can be identified with the adjoint partial differential equations. Since Jameson's pioneering work on the solution of the adjoint flow equations [1], researchers have developed various numerical methods to solve the adjoint flow equations, i.e. potential, Euler or RANS equations, and scientific computing techniques to generate adjoint solver code from a standard flow solver automatically, cf. [2] and references therein.

There are various applications of sensitivity analysis, the most prominent being gradient based optimization methods. The classical gradient descent methods calculate the next design configuration from the gradient of the cost functional and an approximate Hessian. The approximation of the Hessian is updated by each gradient information. Examples of such strategies for optimization without constraints are the Broyden-Fletcher-Goldfarb-Shanno (BFGS) method, and in case there are constraints, the method of Sequential Quadratic Programming (SQP). Moreover, there exist gradient assisted optimization methods which are not based on gradient descent. Surrogate models as introduced e.g. in [3] and [4] are trained by the evaluation of both the functional itself and its sensitivities. A further promising application of adjoint methods are error estimates, cf. [5–7], and the CFD based specification of manufacturing and wear-and-tear tolerances, cf. [8].

The above applications have in common that the functions whose derivatives are calculated are a composition of various process tools, as depicted in Fig. 1. Adjoining the whole process chain can be viewed as evaluating the chain rule in reverse order. One starts from the right and translates, step by step, the sensitivity of the objective functional w.r.t. the flow solution into one w.r.t. the design parameter. If blade and mesh generation are not available in adjoint mode, one has to calculate their derivatives in forward mode, for instance by repeated evaluations with perturbed parameters. One can still obtain the tremendous acceleration of adjoint methods if one applies it to the flow solver which, in the forward approach, is by far the most time consuming.

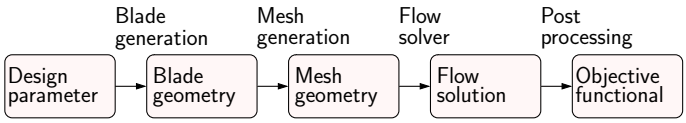

Figure 1. PROCESS CHAIN OF SENSITIVITY CALCULATION

That said, it is indispensible to be able to treat the rightmost function in Fig. 1 in adjoint mode in order to apply adjoint methods. Consequently, one of the subtleties in the development of adjoint solvers is the fact that for each objective functional one has to implement a special right-hand side for the adjoint system. Moreover, if one is interested in gradients that agree with the gradients of the flow solver output then the exact *post-processing* functions have to be considered and their linearization must be used in the *pre-process* of the adjoint solver.

In turbomachinery, the objective functionals, such as mass flow or efficiency, are often evaluated on the boundary of the flow domain, i.e. at the inlets or outlets of the configuration. In the adjoint flow equations, these functionals result in inhomogeneous boundary conditions. In many applications, however, it is important to use arbitrary analysis surfaces away from the boundaries of the computational domain, e.g. when considering the performance of one single blade row in a multi-stage turbomachinery configuration. In that case it might be desirable to place the numerical measurement plane away from the numerical boundaries where boundary conditions cause small spurious reflections that interfere with the solution. On the other hand, the interaction with other rows should be taken into account even if one is primarily interested in the performance of a single blade row.

This article describes how to extend the adjoint solver presented in [9] for objective functionals on arbitrary analysis surfaces. It is explained how to specify the analysis surfaces and how to compute averaged flow quantities on them. Then the generalizations needed in the adjoint code are discussed. Finally, the new methods are validated on the basis of a transonic compressor stage.

THE FLOW SOLVER AND ITS ADJOINT

The adjoint solver used in this article and its underlying flow solver are part of the Reynolds-averaged Navier Stokes (RANS) solver TRACE, developed at DLR for internal flows, especially in turbomachinery [9]. Alongside the research at DLR, the solver is used and developed at several universities, and employed at MTU Aero Engines in the aerodynamic design of components.

Finite Volume Discretization of the RANS Equations

The equations used to model turbomachinery flows are the compressible RANS equations which may be written in the form

$$\frac{\partial q}{\partial t} + \operatorname{div}[F^c(q) + F^v(q)] - S(q) = 0. \tag{1}$$

Here $q = (\rho, \rho U, \rho E)$ denotes the flow field of conservative variables, i.e. density, momentum and total energy. F^c and F^v denote convective and viscous fluxes, respectively. As is common practice in turbomachinery CFD, the flow equations are formulated in the rotating frame of reference. Therefore, S is the source term which accounts for coriolis and centrifugal forces. The effects of turbulence are described using Wilcox's two-equation turbulence model [10].

The finite volume discretization of Eqn. (1) reads

$$\frac{\partial q_i}{\partial t} + V_i^{-1} \sum_{j \in \partial i} F_j(q) - S_i(q) = 0,$$

where q_i denotes the average state in the i-th cell, ∂i the set of its faces, and F_j is the numerical flux at the j-th face. $S_i(q)$ is an approximation of the source term, averaged over the cell whose volume is denoted by V_i. Defining the residual by

$$R_i = V_i^{-1} \sum_{j \in \partial i} F_j(q) - S_i(q), \tag{2}$$

the steady equations read

$$R_i(q, x) = 0, \tag{3}$$

where the dependency of the residual on both the discrete flow variables and the mesh coordinates is emphasized.

Numerical Boundary Conditions

Boundary conditions are imposed by extrapolating the state values at inner cells to so-called dummy cells and calling special flux functions at the bounding faces [11]. At solid walls, slip and no-slip boundary conditions are available. For coarse meshes, wall functions can be used.

At entry, exit and interface boundaries between blade rows, nonreflecting boundary conditions, cf. [12], are applied to the circumferential fluctuations. The circumferentially mixed out states are given by a radial distribution of stagnation temperature, stagnation pressure and flow angles at the entry. At exits the radial distribution of pressure is prescribed or, otherwise, the pressure distribution is computed from the user-specified pressure at midspan and the equation of radial equilibrium.

Adjoint Solver

Suppose that the geometry is parametrized by an f-dimensional vector of design parameters α. Under the assumption that this parametrization and the mesh generation is at least differentiable, the mesh coordinates are differentiable functions of α. If one is interested in the sensitivity of an objective function $I(x, q)$ under variations of α, then the *forward* approach is to solve Eqn. (3) for many different α and to evaluate $I(x, q)$. In fact, Eqn. (3) is an implicit definition of $q(\alpha)$.

Differentiation w.r.t. α_j yields the forward linear problem

$$\frac{\partial R}{\partial q}\frac{\partial q}{\partial \alpha_j} + \frac{\partial R}{\partial x}\frac{\partial x}{\partial \alpha_j} = 0. \tag{4}$$

Given the solution $\frac{\partial q}{\partial \alpha_j}$ to Eqn. (4), the sensitivity can be computed using

$$\frac{\partial}{\partial \alpha_j} I(x(\alpha), q(\alpha)) = \frac{\partial I}{\partial x}\frac{\partial x}{\partial \alpha_j} + \frac{\partial I}{\partial q}\frac{\partial q}{\partial \alpha_j}. \tag{5}$$

In order to explain the adjoint method, the second summand is rewritten using Eqn. (4),

$$\begin{aligned} \frac{\partial I}{\partial q}\frac{\partial q}{\partial \alpha_j} &= \left(\left(\frac{\partial I}{\partial q}\right)^T\right)^T \frac{\partial q}{\partial \alpha_j} \\ &= -\left(\left(\frac{\partial I}{\partial q}\right)^T\right)^T \left(\frac{\partial R}{\partial q}\right)^{-1} \frac{\partial R}{\partial x}\frac{\partial x}{\partial \alpha_j} \\ &= -\underbrace{\left(\left(\left(\frac{\partial R}{\partial q}\right)^T\right)^{-1} \left(\frac{\partial I}{\partial q}\right)^T\right)^T}_{=:\psi} \frac{\partial R}{\partial x}\frac{\partial x}{\partial \alpha_j}. \end{aligned} \tag{6}$$

This definition of the *adjoint solution* ψ can be translated into the linear equation

$$\left(\frac{\partial R}{\partial q}\right)^T \psi = \left(\frac{\partial I}{\partial q}\right)^T. \tag{7}$$

Summarizing, one can calculate the sensitivity of I w.r.t. α_j using

$$\frac{\partial}{\partial \alpha_j} I(x(\alpha), q(\alpha)) = \frac{\partial I}{\partial x}\frac{\partial x}{\partial \alpha_j} - \psi^T \frac{\partial R}{\partial x}\frac{\partial x}{\partial \alpha_j}. \tag{8}$$

Given ψ, the computational effort to evaluate the sensitivity for many design parameters reduces dramatically since the calculation of the sensitivities w.r.t. the mesh geometry is rather cheap. Since the conditions of the linear operators $\left(\frac{\partial R}{\partial q}\right)^T$ and $\frac{\partial R}{\partial q}$ are identical, solving the adjoint equations is approximately as difficult as solving the steady equations for a small change of α.

The adjoint solver in TRACE solves the discrete adjoint equations, i.e. the left-hand side in Eqn. (7) is the linearization of the residual R of the steady solver. The exact residual Jacobians are, however, approximated by finite differences. The resulting large sparse block matrix A is stored in compressed row storage format, each entry being a 5×5 submatrix. Transposition leads to the adjoint operator. Similarly, the implementation of the adjoint boundary conditions is also based on the linearization of the corresponding routines of the steady solver. In particular, nonreflecting boundary conditions and the blade row coupling using conservative mixing planes have been linearized and adjoined. For more details, the reader is referred to [9].

The adjoint solver used in this article is based on the so-called constant-eddy-viscosity (CEV) assumption, i.e. when computing sensitivities w.r.t. shape variations, the eddy viscosity takes the same values as for the initial geometry. For the validity of the CEV approximation and its application in automatic optimization, cf. [13, 14].

Solution Methods

The nonlinear system in Eqn. (3) is solved by an implicit pseudo-time marching method. The adjoint equations are solved using a restarted preconditioned GMRES method. The parallelization strategy for both solvers is domain decomposition. The computational work is distributed onto a high performance cluster. In steady mode, ghost cells at block cuts storing copies of cells in neighboring blocks are updated after every internal update. In contrast, the adjoint ghost cell update is called after matrix multiplication in the adjoint solver, cf. [9].

Interpretation of the Adjoint Solution

The adjoint solution ψ is itself difficult to interpret in terms of a variation of the geometry. However, for a given functional I, one can give the adjoint field ψ a precise meaning by considering the sensitivity of I under variations of source terms. Recall from Eqn. (2) that the steady flow is determined by

$$V_i^{-1} \sum_{j \in \partial i} F_j(q) = S_i(q).$$

Now suppose that this system is not perturbed by a variation of the geometry but by the addition of a source field, i. e.

$$V_i^{-1} \sum_{j \in \partial i} F_j(q_\varepsilon) = S_i(q_\varepsilon) + \varepsilon \widetilde{S}_i,$$

where $\widetilde{S}_i$ is a discretized source density and ε a small control parameter. Observe that $\widetilde{S}_i$ corresponds to an average source density. The first variation of q is determined by differentiation w.r.t. ε, hence

$$\frac{\partial R}{\partial q}\frac{\partial q_\varepsilon}{\partial \varepsilon} = \widetilde{S}.$$

The first variation of the objective functional $I(q)$ is therefore given by

$$\begin{aligned} \frac{\partial I(q_\varepsilon)}{\partial \varepsilon} &= \frac{\partial I}{\partial q}\frac{\partial q_\varepsilon}{\partial \varepsilon} \\ &= \frac{\partial I}{\partial q}\left(\frac{\partial R}{\partial q}\right)^{-1}\widetilde{S} \\ &= \psi^T \widetilde{S} \\ &= \sum_i (V_i^{-1}\psi_i)^T \widetilde{S}_i V_i. \end{aligned} \tag{9}$$

Here, the cell volume has been introduced in order to write the sensitivity as a weighted sum of the sources integrated over one cell, $\widetilde{S}_i V_i$. The components of $\widetilde{S}_i V_i$ correspond to mass flow, momentum flux and energy flux, respectively, of the source added. One deduces from Eqn. (9) that the components of the modified adjoint solution $V_i^{-1}\psi_i$ can be interpreted as the sensitivity of the objective functional I w.r.t. a source in the corresponding component at the i-th cell. In particular the SI units of $V_i^{-1}\psi_i$ are given by

$$[V_i^{-1}\psi_i^{(1)}] = [I] \cdot \frac{s}{kg}, \tag{10}$$

$$[V_i^{-1}\psi_i^{(2,3,4)}] = [I] \cdot \frac{1}{N}, \tag{11}$$

$$[V_i^{-1}\psi_i^{(5)}] = [I] \cdot \frac{1}{W}, \tag{12}$$

where $[I]$ is the unit of the objective functional. E.g., when I is mass flow, then the adjoint density $V_i^{-1}\psi_i^{(1)}$ is a dimensionless field.

It follows that the modified adjoint field $V_i^{-1}\psi_i$ has a physical meaning which is independent of the mesh under consideration. Consequently, the plots of adjoint solution fields in this article refer to the modified adjoint field.

OBJECTIVE FUNCTIONALS AND ADJOINT FORMULATION

Although some functions for turbomachinery performance are based on volume integrals, e.g. entropy production, cf. [15], most common objective functionals are based on surface integrals

$$I(x,q) = \int_\Gamma h(x,q)dS(x), \tag{13}$$

for some function h and analysis surface Γ.

Functionals Defined at the Blade Geometry

Typical functionals to assess the performance of an airfoil are lift and drag. Similarly, open rotors constitute a turbomachinery application where integrals over the blade surface are used, e.g. to calculate thrust from pressure and shear stresses over the blade. Consequently, applications of adjoint solvers to external flows typically use an analysis surface Γ which is identical with the boundary to be optimized. This implies a direct dependency of I on the blade geometry as an additional ingredient in the sensitivity calculation, in contrast to the adjoint methods presented in [9].

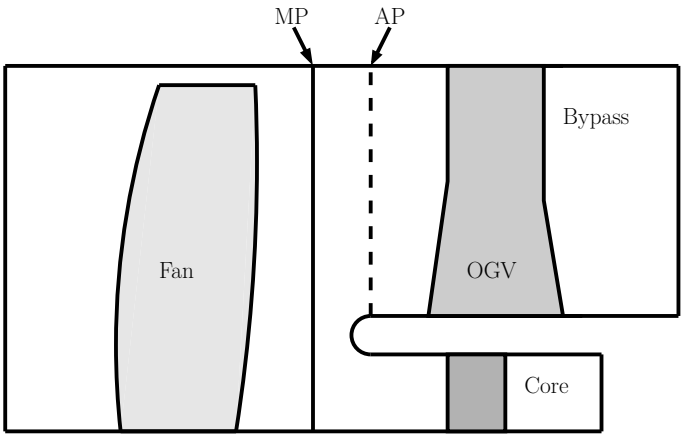

Figure 2. COMPUTATIONAL DOMAIN CONSISTING OF FAN, OGV AND CORE IGV WITH ANALYSIS PLANE (AP) AND MIXING PLANE (MP).

Functionals Defined at Surfaces away from Varying Boundaries

In turbomachinery CFD, it is common practice to evaluate stagnation pressure and temperature ratio between two axial positions. The flow solver considered in this article allows for the specification of two kinds of such analysis surfaces. Of the first kind are surfaces that are boundaries of the computational domains, i.e. either inlets, outlets or the interfaces between blade rows. The second class of surfaces consists of isosurfaces of general channel coordinates that parametrize the annulur channel, e.g. relative channel length and height. The channel coordinates, in turn, are specified by the user.

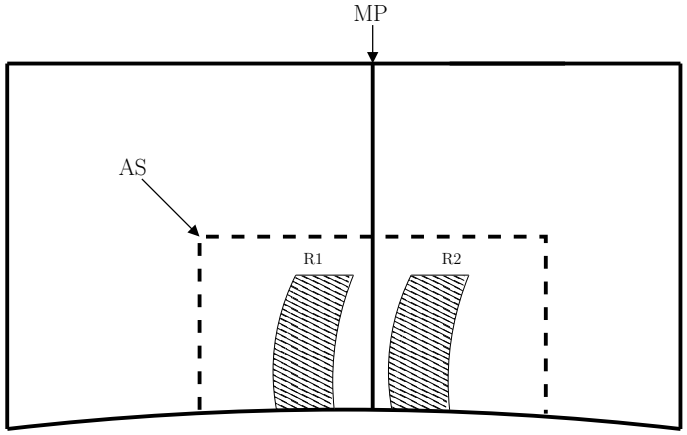

Figure 3. COMPUTATIONAL DOMAIN FOR OPEN ROTOR CONFIGURATION WITH ANALYSIS SURFACE (AS) AND MIXING PLANE (MP).

Fig. 2 shows the configuration of a fan with outlet guide vane (OGV) and part of the core. In order to evaluate the total pressure losses of the OGV, one would like to place an analysis surface between the tip of the splitter and the leading edge of the OGV. An interior analysis surface might also be useful when considering an open rotor configuration. Thrust and specific work of the rotors can be obtained by surface integrals of the momentum and energy flux over a rotational analysis surface as depicted in Fig. 3.

The flow solver environment TRACE allows for the generation of analysis surfaces as a preprocess. The preprocessing tool that assembles the analysis surfaces uses the VTK library [16] to generate auxiliary surface meshes that represent the user-specified isosurfaces. Each grid computed by VTK consists of triangles which represent the intersection of one cell of the volume mesh with the isosurface. Therefore, the (online) post processing tools can interpolate the flow solution to the triangles very efficiently and, subsequently, perform various kinds of averages, circumferential Fourier decompositions, etc.

Functionals Defined by Radial Distributions

It is important to control not only global, averaged flow parameters but also radial distributions, especially for design and optimization of blade rows in a multi-stage engine. For instance, when optimizing the isentropic efficiency of a stage, a typical constraint is that the radial distribution of the circumferential out-

flow angle α be fixed. To treat such a constraint in adjoint mode, one may consider the outflow angle at several radial heights. However, the adjoint approach is inefficient if many functionals are considered simultaneously. Therefore it is suggested to employ the mean square deviation of flow parameters such as outflow angles from target distributions β^*, i.e.

$$I(q) = \int_{r_{\mathbf{hub}}}^{r_{\mathbf{tip}}} (\beta(r) - \beta^*(r))^2 w(r) dr, \tag{14}$$

for some radial weighting function $w(r)$. $\beta(r)$ is the flow angle computed from the circumferentially averaged state

$$\overline{q}^F(r) = (F^{\overline{n}})^{-1}\Big(\frac{1}{2\pi}\int_0^{2\pi} F^n(q) d\vartheta\Big).$$

Here, it is preferable to calculate the flow angle from the circumferentially mixed-out state $\overline{q}^F(r)$, since, using conservative mixing-planes [17], $\overline{q}^F(r)$ determines the radial distribution of inflow angles in the next blade row.

Linearization of the Functionals

According to Eqn. (7), one has to differentiate the various objective functionals, in order to calculate the right-hand side of the adjoint solver. To explain this in detail, consider an objective functional I which is a function of the flux averages over several analysis surfaces $\Gamma_1, \Gamma_2, \ldots$, i.e.

$$I(q) = I(\overline{q}_1^F, \overline{q}_2^F, \ldots). \tag{15}$$

Here, the flux average [18] (or mixed-out state) is defined by

$$\overline{q}_i^F = \big(F^{\overline{n}}\big)^{-1}\Big(\frac{1}{|\Gamma_i|}\int_{\Gamma_i} F^n(q)\, dS\Big). \tag{16}$$

F^n denotes the convective flux in the direction of the normal vector n. $\overline{n}$ denotes the surface averaged normal. Note that different averages such as the so-called work average, the availability or entropy average, etc. can be written in the same form, but with a different flux function F^n, cf. [19]. The following derivation of adoint right-hand sides carries over verbatim to other averaging techniques.

Using Eqns. (15) and (16), the linearization of I w.r.t. the flow quantities is given by

$$\delta I = \frac{\partial I}{\partial q_1}\delta\overline{q}_1^F + \frac{\partial I}{\partial q_2}\delta\overline{q}_2^F + \ldots, \tag{17}$$

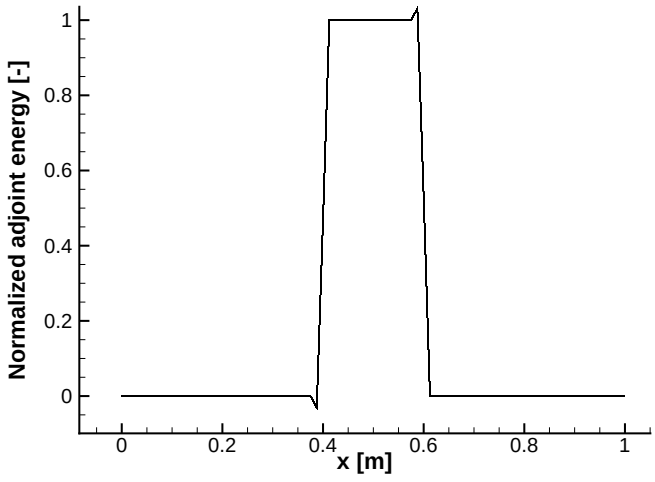

Figure 4. ADJOINT SOLUTION (ENERGY) FOR TOTAL TEMPERATURE RATIO BETWEEN TWO INTERIOR ANALYSIS SURFACES.

where the linearized flux average is given by

$$\delta\overline{q}_i^F = \big(DF^{\overline{n}}|_{\overline{q}_i^F}\big)^{-1}\Big(\frac{1}{|\Gamma_i|}\int_{\Gamma_i} DF^n|_q \delta q\, dS\Big). \tag{18}$$

Here, $DF^n|_q$ denotes the flux Jacobian at q. In order to linearize exactly the implementation of the forward post-process the specific discretization of the surface integral in Eqn. (16) has to be taken into account. Together with the coefficients of the interpolation from the cells onto the above-mentioned triangles, this yields $\frac{\partial I}{\partial q_i}$ for the i-th cell.

Mean square deviations may be linearized in a similar manner. For instance, linearizing Eqn. (14) yields

$$\delta I(q) = 2\int_{r_{\mathbf{hub}}}^{r_{\mathbf{tip}}} (\beta(r) - \beta^*(r))\delta\beta(r) w(r) dr. \tag{19}$$

Using

$$\delta\beta(r) = \frac{\partial\beta}{\partial q}\Big|_{\overline{q}^F}\delta\overline{q}^F(r)$$

and Eqn. (18) for the linearization of flux averages, one obtains $\frac{\partial I}{\partial q}$ for the functional defined in Eqn. (14).

To verify the implementation, we consider the constant axial flow in a duct. The adjoint Euler solution for the stagnation temperature ratio between two interior analysis planes at 40% and 60% channel length is calculated. Since in the steady setup, the stagnation temperature at the inlet is given by the boundary

condition, it is straightforward to calculate the adjoint energy. Stagnation temperature is proportional to the stagnation enthalpy, which in turn is the energy flux per mass flow. Recall from (9) that the adjoint energy at x is the sensitivity of the stagnation temperature ratio w.r.t. an energy source at x, say $\widetilde{S}^{(e)}$. Labelling the x-positions and flow quantities at the analysis surfaces by 1 and 2, one has

$$\delta\vartheta_{\mathbf{t}} = \begin{cases} \frac{\widetilde{S}^{(e)}}{c_p T_{\mathbf{t},1}\dot{m}}, & \text{if } x_1 < x < x_2 \\ 0, & \text{otherwise.} \end{cases}$$

It follows that the normalized adjoint energy

$$\hat{\psi}_i^{(e)} = c_p T_{\mathbf{t},1}\dot{m}V_i^{-1}\psi_i$$

is the characteristic function of the interval $[x_1, x_2]$. The adjoint energy computed with the discrete adjoint solver is depicted in Fig. 4. It coincides with the analytic solution up to small numerical artefacts close to the jumps at the analysis surfaces. The latter, however, are of minor interest for applications, since mesh perturbations are expected to be smooth, especially near the analysis surface.

TURBOMACHINERY APPLICATION

The Test Case

The Darmstadt Transonic Compressor test rig has been operated since 1993. Several experimental data for three different rotor designs are available. As shown in [20], mass flow and efficiency prediction by the nonlinear solver are in very high agreement with experimental data. To test the new functionals in the adjoint solver, the baseline rotor geometry (Rotor No.1, cf. [21]) has been chosen.

The numerical setup with hub and blade surfaces as well as an analysis surface is shown in Fig. 5. The block structured mesh contains 200,000 cells and the wall functions are employed at all solid walls. Blade fillets have not been resolved. The analysis surface corresponds to the intersection of the computational domain with an axial plane between the mixing-plane and the stator. Non-reflecting boundary conditions and the conservative mixing-plane approach have been used at the inlet, outlet and interface between rotor and stator. The operating point considered here is at a mass flow of 16.2 kg/s and a stagnation pressure ratio of 1.49.

The Design Space

To test the numerical methods presented in this paper, an eight-dimensional design space has been considered. The radial

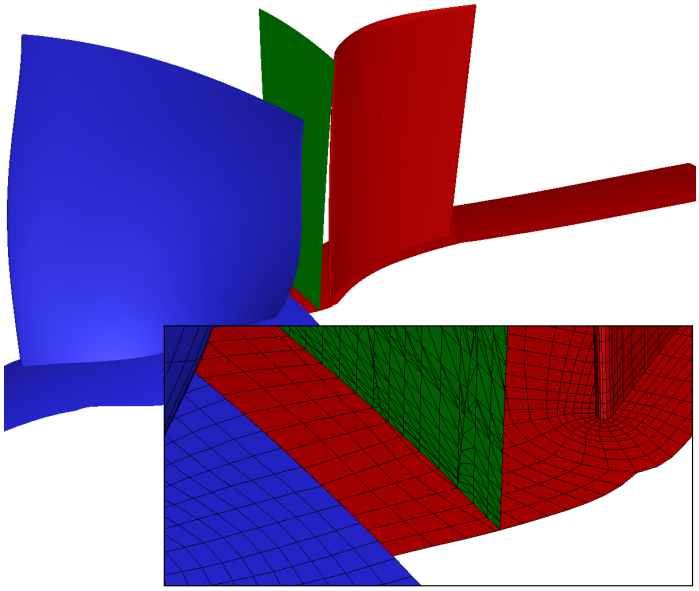

Figure 5. ROTOR STATOR CONFIGURATION WITH MESH DETAILS AND ANALYSIS SURFACE.

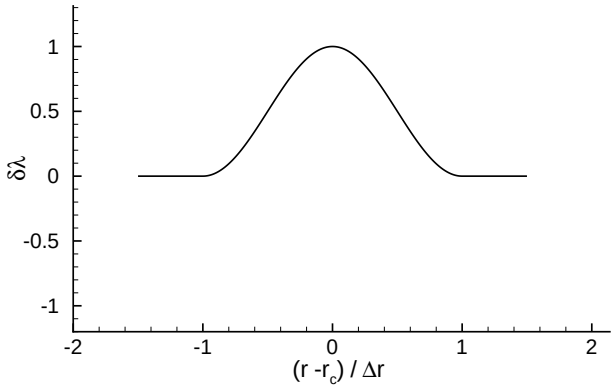

Figure 6. RADIAL BUMP FUNCTION USED TO RESTAGGER BLADE SECTIONS.

distribution of the stagger angles is modified by a small multiple of a bump function in r, plotted in Fig. 6. More precisely,

$$\delta\lambda(r) = \begin{cases} \cos^2\left(\frac{\pi}{2}\frac{r-r_c}{\Delta r}\right), & \text{if } |r-r_c| < \Delta r, \\ 0, & \text{otherwise.} \end{cases}$$

For the j-th design parameter, the radial height of the restaggering is defined by

$$r_c = 0.12\text{m} + (j-1)\Delta r, \quad j = 1,...,8,$$

and $\Delta r = 0.01\text{m}$.

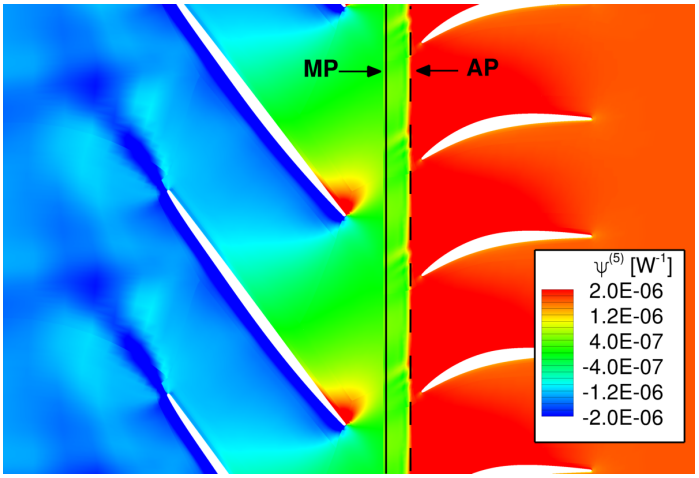

Figure 7. ENERGY COMPONENT OF ADJOINT SOLUTION FOR STAGNATION PRESSURE RATIO BETWEEN INLET AND ANALYSIS PLANE (AP).

Sensitivity Analysis

As a reference for the adjoint solver, the sensitivities of various flow parameters have been calculated in forward mode. Since the adjoint solver is based on the CEV approximation, the sensitivities have been calculated both with and without the turbulence model. More precisely, the steady solver has been run in CEV mode, i.e. the turbulence quantities are read from the converged steady solution of the initial geometry, but are not updated by the turbulence model. The CEV sensitivities therefore provide, on the one hand, an exact reference for the adjoint solver and, on the other, can be used to assess the validity of the CEV approximation itself.

The sensitivities of the following five objective functionals have been calculated in adjoint and steady mode:

Objective functional	Location of evaluation
Mass flow	Outlet
Stagnation pressure ratio	Inlet, outlet
Stagnation pressure ratio	Inlet, analysis surface
Outflow angle β	Analysis surface
Mean sqare deviation of β from β^*	Rotor-stator interface.

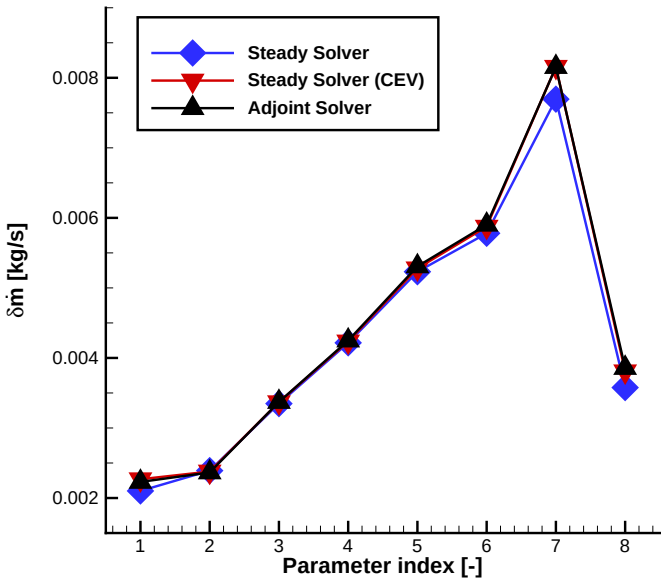

Figure 8. SENSITIVITIES OF MASS FLOW.

For simplicity, the target distribution of the circumferential outflow angle, β^*, has been set to 0. In order to guarantee close to linear dependence of the functionals, the blade sections have been restaggered by only 0.1 degrees. It is crucial to verify that the differences in the five functionals are sufficiently large in order to avoid relative errors due to the finite accuracy of floating point arithmetic.

Fig. 7 shows the adjoint solution for the third functional, which is proportional to the mixed-out stagnation pressure at the analysis surface, as the inlet stagnation pressure is fixed by the boundary condition. As in the solution to the beforementioned numerical test (cf. Fig. 4), one observes a jump across the analysis plane.

Results

Fig. 8 and 9 show the sensitivities for the mass flow and the two stagnation pressure ratios, respectively. The agreement of the adjoint results with those computed in CEV mode are nearly perfect. When the influence of the turbulence model is taken into account, the sensitivities differ somewhat but are still promising. The CEV and non-CEV results coincide not only in sign and magnitude, but also in their trend w.r.t. the radial position of the restaggering.

From Fig. 9, one deduces that the sensitivities of stage and rotor stagnation pressure ratio are similar but differ by the effect of a change in stator losses. The fact that the corresponding adjoint sensitivities are in very good agreement with the steady results demonstrates that the adjoint solver is also capable of

resolving the comparatively small influence of the restaggering of the rotor sections onto the stator losses. As can be seen in the plots in Fig. 10, both the sensitivity of the circumferential flow angle at the analysis plane and the mean square deviation of it from a given distribution can be calculated using the adjoint solver. The results show that the influence of the turbulence model is small at midspan and increases towards hub and blade tip.

Computational Efficiency

It took the adjoint solver between 1.1 and 1.25 CPU hours to reduce the L^2-residual by 4 orders of magnitude on an Intel E5440 Xeon cluster. The steady calculations for the forward computations have been initialized with the steady solution of the unperturbed geometry and terminated after the reduction of the residual by about 5 orders of magnitude. This took approximately 1.25 CPU hours in CEV mode and about 1.45 CPU hours in conventional mode. Summarizing, the convergence speed of the adjoint solver is not affected by the location of the objective functional and is very similar to that of the steady solver.

CONCLUSIONS

To apply adjoint methods in turbomachinery CFD, one has to accomodate complex post processing functionals. To achieve this, the adjoint solver has been extended to include functionals

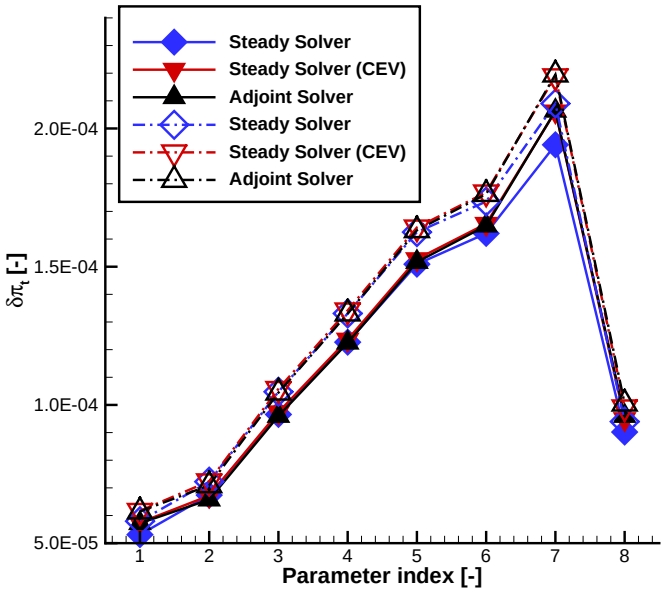

Figure 9. SENSITIVITIES OF STAGNATION PRESSURE RATIO. SOLID LINES: STAGE RATIO. DASHED LINES: RATIO BETWEEN INLET AND ANALYSIS PLANE.

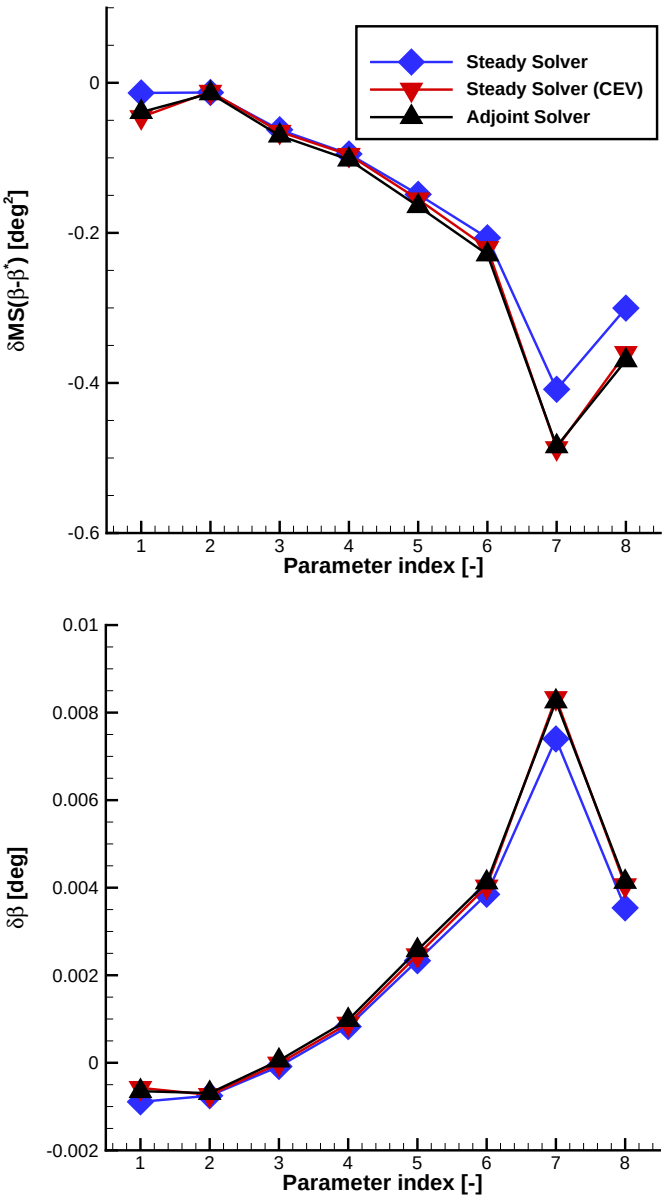

Figure 10. SENSITIVITIES OF CIRCUMFERENTIAL FLOW ANGLE. ABOVE: MEAN SQUARED DEVIATION FROM TARGET DISTRIBUTION AT INTERFACE. BELOW: MIXED-OUT ANGLE AT ANALYSIS PLANE.

defined on arbitrary analysis surfaces. The necessary modifications to the right-hand side of the adjoint solver have been outlined and implemented in an existing adjoint three-dimensional RANS solver.

The methods have been validated by means of variations of the blade geometry in a transonic compressor stage. The results show that the underlying discrete adjoint solver, together with the

generalizations proposed in this article, calculates sensitivities that are in nearly perfect agreement with sensitivities obtained from the steady solver. Whereas the CEV assumption provides excellent results at midspan, it shows small but noticeable deviations from the fully turbulent sensitivities close to hub and tip where the flow is highly three-dimensional.

REFERENCES

[1] Jameson, A., 1988. "Aerodynamic design via control theory". *Journal of Scientific Computing,* ***3***(3), pp. 233–260.

[2] Giles, M. B., and Pierce, N. A., 2000. "An introduction to the adjoint approach to design". *Flow, Turbulence and Combustion,* ***65***, pp. 393–415.

[3] Giannakoglou, K., Papadimitriou, D., and Kampolis, I., 2006. "Aerodynamic shape design using evolutionary algorithms and new gradient-assisted metamodels". *Computer Methods in Applied Mechanics and Engineering,* ***195***(44-47), pp. 6312 – 6329.

[4] Bompard, M., Peter, J., and Désidéri, J.-A., 2010. "Surrogate models based on function and derivative values for aerodynamic global optimization". V European Conference on Computational Fluid Dynamics ECCOMAS CFD 2010, Lisbon, Portugal.

[5] Giles, M. B., and Süli, E., 2002. "Adjoint methods for PDEs: a posteriori error analysis and postprocessing by duality". *Acta Numerica,* ***11***(-1), pp. 145–236.

[6] Venditti, D. A., and Darmofal, D. L., 2002. "Grid adaptation for functional outputs: Application to two-dimensional inviscid flows". *Journal of Computational Physics,* ***176***(1), pp. 40 – 69.

[7] Venditti, D. A., and Darmofal, D. L., 2003. "Anisotropic grid adaptation for functional outputs: application to two-dimensional viscous flows". *Journal of Computational Physics,* ***187***(1), pp. 22 – 46.

[8] Ghate, D., and Giles, M., 2006. *Inexpensive Monte Carlo uncertainty analysis*. Tata McGraw-Hill, New Delhi, pp. 203–210.

[9] Frey, C., Nürnberger, D., and Kersken, H.-P., 2009. "The discrete adjoint of a turbomachinery RANS solver". ASME Paper GT2009-59062.

[10] Wilcox, D. C., 2006. *Turbulence modeling for CFD*, 3rd ed. DCW Industries, La Cañada, USA.

[11] Blazek, J., 2001. *Computational fluid dynamics: Principles and applications*. Elsevier, Amsterdam.

[12] Giles, M. B., 1990. "Non-reflecting boundary conditions for euler calculations.". *AIAA J.,* ***28***(12).

[13] Dwight, R., and Brezillon, J., 2006. "Effect of approximations of the discrete adjoint on gradient-based optimization". *AIAA Journal,* ***44***(12), pp. 3022–3071.

[14] Kim, C. S., Kim, C., and Rho, O. H., 2003. "Feasibility study of constant eddy-viscosity assumption in gradient-based design optimization". *Journal of Aircraft,* ***40***(6), pp. 1168–1176.

[15] Papadimitriou, D., Zymaris, A., and Giannakoglou, K. "Discrete and continuous adjoint formulations for turbomachinery applications". EUROGEN 2005, Munich, September 12-14, 2005.

[16] Schroeder, W., Martin, K., Martin, K., and Lorensen, B., 1998. *The visualization toolkit*. Prentice Hall PTR.

[17] Denton, J., and Singh, U., 1979. "Time marching methods for turbomachinery flow calculations". In VKI Lecture Series 1979-7, von Karman Institute.

[18] Greitzer E. M., Tan C. S. and Graf M. B., 2004. *Internal Flow*. Cambridge Univ. Press, New York.

[19] Cumpsty, N. A., and Horlock, J. H., 2006. "Averaging nonuniform flow for a purpose". *Journal of Turbomachinery,* ***128***(1), pp. 120–129.

[20] Yang, H., Nürnberger, D., Kügeler, E., 2007. "Recent progress in the hybrid-grid CFD simulation of turbomachinery flows". ISABE Paper 2007-1231.

[21] Schulze G., Hennecke D.K., Sieber J., Wöhrl B., 1994. "Der neue Verdichterprüfstand an der TH Darmstadt". *VDI Berichte Nr. 1109, Germany.*